Acknowledgment

The authors gratefully acknowledge the assistance of T. Hyltin, who originally suggested this technique to the authors and contributed many helpful suggestions.

References

[1] N. Houlding, "Measurement of varactor quality," *Microwave J.*, vol. 3, pp. 40–45, January 1960.
[2] R. I. Harrison, "Parametric diode Q measurements," *Microwave J.*, vol. 3, pp. 43–46, May 1960.
[3] W. E. Doherty, Jr., "Precise cutoff frequency characterization of varactor diodes," presented at the 1966 Internat'l Solid-State Circuits Conf., Philadelphia, Pa.
[4] B. C. DeLoach, "A new microwave measurement technique to characterize diodes and an 800-Gc cutoff frequency varactor at zero volts bias," *IEEE Trans. on Microwave Theory and Techniques*, vol. MTT-12, pp. 15–20, January 1964.
[5] D. A. E. Roberts and K. Wilson, "Evaluation of high quality varactor diodes," *1965 Proc. Joint Symp. on Microwave Applications of Semiconductors*, University College, London, England.
[6] F. J. Hyde, S. Deval, and C. Toker, "Varactor diode measurements," *1965 Proc. Joint Symp. on Microwave Applications of Semiconductors*, University College, London, England.
[7] W. E. Wells, Jr., J. C. Sadler, S. A. Robinson, and W. P. Waters, "Planar Schottky barrier microwave mixers and varactors in gallium arsenide," presented at the 1965 Electron Devices Meeting, Washington, D.C.
[8] W. J. Getsinger, "The packaged and mounted diode as a microwave circuit," *IEEE Trans. on Microwave Theory and Techniques*, vol. MTT-14, pp. 58–69, February 1966.
[9] F. Bolinder, "Fourier transforms in the theory of inhomogeneous transmission lines," *Trans. Roy. Inst. Tech. (Stockholm, Sweden)*, 1951.
[10] D. A. E. Roberts, "Measurements of varactor diode impedance," *IEEE Trans. on Microwave Theory and Techniques (Correspondence)*, vol. MTT-12, pp. 471–475, July 1964.
[11] N. Houlding, "Varactor measurements and equivalent circuits," *IEEE Trans. on Microwave Theory and Techniques (Correspondence)*, vol. MTT-13, pp. 872–873, November 1965.

A Positive Resistance Up-Converter for Ultra-Low-Noise Amplification

E. SARD, MEMBER, IEEE, B. PEYTON, MEMBER, IEEE, AND S. OKWIT, FELLOW, IEEE

Abstract—**An ultra-low-noise two-channel tunable amplifier system, operating in the 1.5 to 2.5 GHz frequency range, consisting of a cooled positive resistance parametric up-converter followed by a traveling-wave maser (TWM) and down-converter, has been developed. A theoretical analysis of the important operating and design parameters of the up-converter is presented and experimentally verified. Experimental data is given on the operation of the up-converter with the input and output ports reversed (down-converter), and is shown to correlate with the theoretical model.**

A brief discussion is presented on the TWM, and the spurious signal considerations which govern the choice of maser center frequency (up-converter output frequency). Finally, some preliminary system data is given showing the low noise performance of the overall cascaded amplifier integrated with a 4.2°K closed-cycle refrigerator.

I. Introduction

A. General

DURING the past few years the technology of ultra-low-noise amplifiers has been in a dynamic growth stage. The impetus to this growth has been the constantly increasing activity in applications such as satellite communications, deep space communications, telemetry, and radio astronomy.

Two amplifier configurations that have been actively competing for use in these systems are the traveling-wave maser (TWM) and the cooled one-port parametric amplifier. The selection of one of these amplifiers for a given application has created many thought-provoking questions and controversies concerning trade offs in operating characteristics, complexity, cost, and the like. There are so many parameters that enter into the selection that it is almost impossible to present a simple set of criteria that will yield a satisfactory rule for the optimum choice.

The advantages associated with the traveling-wave maser and the parametric amplifier are relatively well-known. For example, the maser provides:

1) the ultimate in low-noise performance,
2) excellent stability characteristics (by virtue of the relative insensitivity of maser gain to pump power and frequency variations),
3) unconditional gain stability (resulting from isolator elements integrally located in the maser structure),
4) excellent intermodulation distortion characteristics,
5) no burnout problems.

The parametric amplifier, on the other hand, has the well-known advantages of:

1) providing broad instantaneous bandwidths with relative ease (5 to 10 percent),
2) rapid and simple electronic tunability,

Manuscript received June 29, 1966; revised September 7, 1966. This work was supported by the RF System Engineering Section, INS-322, NASA, John F. Kennedy Space Center, Fla.

The authors are with Airborne Instruments Laboratory, Division of Cutler-Hammer, Inc., Melville, N. Y.

3) not requiring an operating environment of liquid helium temperatures (thus avoiding the added complexity of a Joule–Thomson stage in the refrigerator),
4) relative insensitivity of gain in the presence of fluctuations in its physical temperature.

This paper describes a two-channel receiving system that uses a unique cascaded amplifier configuration consisting of a TWM as a second stage preceded by a low-noise two-port positive resistance parametric up-converter. This combination provides the broadband qualities and ease of tunability associated with the parametric amplifier and the ultra-low-noise and stability characteristics associated with the TWM.

B. Cascaded Amplifier Configuration

The amplifier configuration evolved was for a specific application in the 1500 to 2500 MHz region, requiring maser-like noise performance, instantaneous bandwidths of about 70 MHz, and wide tunability. The use of a TWM was precluded for such an application because of the difficulties encountered in realizing broad instantaneous bandwidths simultaneously with wide tunability (which is compounded by the low-frequency range of interest). The use of a conventional cryogenically cooled one-port parametric amplifier was precluded because of the difficulties in achieving a broadband circulator that operates at cryogenic temperatures in this low-frequency range and the resulting degradation the circulator would have on the overall noise performance, gain flatness, and stability.

A block diagram of one of the channels of the cascaded amplifier configuration is shown in Fig. 1. It consists of a widely tunable up-converter that provides low noise with moderate gain over wide frequency bands. The up-converter converts the input frequency (f_1) into a fixed output frequency (f_2) by means of a variable pump frequency (f_p). The output frequency is fed into a magnetically stagger-tuned (broadband) TWM having an approximate bandwidth of about 70 MHz. The output of the maser is then down-converted to the original input frequency by driving a down-converter with the same pump source used for the up-converter. This down-conversion technique eliminates the problems of phase and frequency instabilities.

The advantages of this configuration are numerous, and are described in a latter part of the text. However, one advantage worthwhile pointing out at this time is the versatility of the configuration. Since the converters are relatively small, simple, inexpensive, and easily tunable with a solid-state pump source, "plug-in" converter heads covering different frequency ranges can readily be adapted to the fixed-tuned maser. Thus, there exists the possibility of an amplifier having maser-like noise performance over an extremely broad frequency range at relatively low cost.

The key to the successful realization of the cascaded

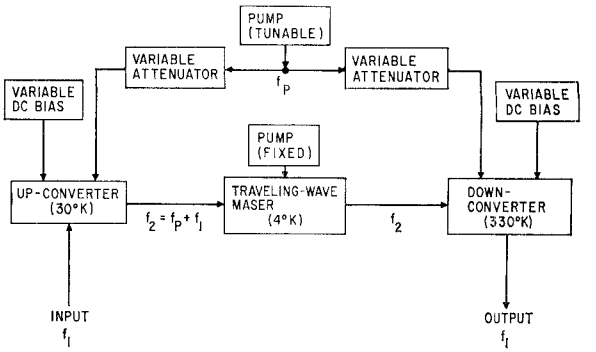

Fig. 1. Block diagram of system (one channel).

configuration is the low-noise up-converter. Consequently, the major portion of this paper will concern itself with the theoretical and experimental aspects of the up-converter design. A brief description of the TWM and the experimental results obtained in the cascaded configuration operating in a 4.2°K closed-cycle refrigerator are also given.

II. Up-Converter and Down-Converter

Some of the features of a tunable parametric up-converter including the effect of varactor losses have been covered in a purely theoretical paper by Matthaei [1]. In this section, his work is extended theoretically, and experimental results are also given. The theoretical extensions include: 1) derivation of the gain over the tuning range and not just at midband, 2) derivation of the effective input noise temperature over the tuning range, 3) discussion of the effect of, and optimization of, the unpumped input SWR on gain, noise temperature, and tunability, and 4) derivation of the gain and noise temperature for operation as a down-converter.

A. Description

Figure 2 shows a lumped equivalent circuit of a balanced varactor up-converter. The particular balanced configuration shown inherently isolates the signal input port from both the sum output and pump ports. The latter two ports are isolated from each other by the band-reject and high-pass filters shown. Additional features include: 1) single-tuning and impedance transformation at signal input and sum output frequencies, 2) broadband single-tuning at the pump frequency, and 3) provision for dc biasing of the varactors. To operate the unit as a down-converter requires only interchanging the roles of the "signal in" and "sum out" ports.

Figure 3 shows the interior details of a balanced up-converter as constructed. The GaAs varactors (modified Sylvania type D5047B) are mounted in series across a double-ridge waveguide dimensioned to accommodate just the bodies of the varactors. Additional features not specifically labeled corresponding to the equivalent circuit of Fig. 2 are: 1) the reduced-height rectangular waveguide at the sum-port side of the unit, which serves both as the high-pass filter and sum transformer (ad-

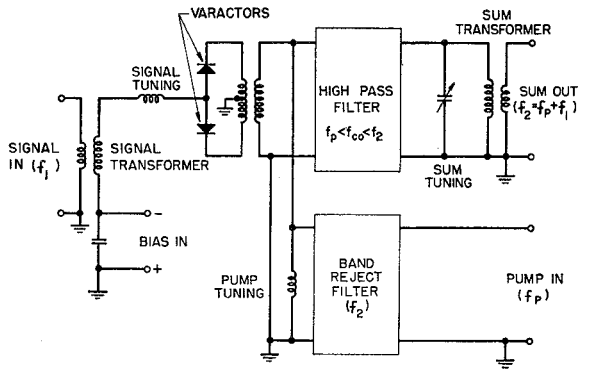

Fig. 2. Lumped equivalent circuit of balanced varactor up-converter.

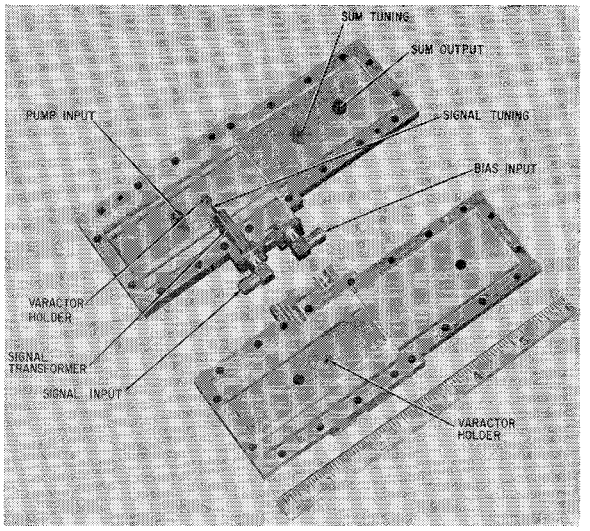

Fig. 3. Breadboard up-converter.

justed for a near match at midband), 2) the location of the pump-port transition a half-wavelength at the sum frequency from the end wall of the ridge waveguide, which serves as the band-reject filter, and 3) the proper location of the junction between the ridge and rectangular waveguides, which serves as the pump tuning. Converters for the two frequency channels are identical except in their integrated signal-bias circuits. All converter development was done at room temperature; subsequent operation of the up-converter units in the 20 to 30°K range was accomplished solely by adjusting the bias and pump power applied to the varactors.

B. Theory and Measurements

General theoretical expressions for the power gain (both available and transducer) and the effective input noise temperature of the up-converter vs. signal input frequency are derived in Appendix I [see (16), (26), and (17), respectively]. Although the derivations are implicit for a single varactor design, they apply equally well to the balanced design of Fig. 2, assuming identical varactors. The actual unpumped SWR at signal input and sum output ports must be used in the formulas, however, considering that the varactors are in parallel at the signal input frequency, and in series at the sum output frequency. The previous general expressions simplify greatly in the middle of the tuning range [see (18), (28), and (19) respectively].

Generally different optimum values of the unpumped input SWR (which depends on the signal input transformation) exist to maximize the midband available power gain or to minimize the midband effective input noise temperature. These optimum values are, respectively, (20) and (21):

$$(S_1)_{\text{opt, 1}} = \sqrt{\frac{M^2}{f_{10}f_{20}} + 1}$$

$$(S_1)_{\text{opt, 2}} = \sqrt{\frac{M^2}{f_{10}^2} + 1} > (S_1)_{\text{opt, 1}}.$$

It is seen that the smaller the frequency ratio f_{20}/f_{10}, the smaller the difference between the two optima. The resultant maximum gain and minimum noise temperature are (22) and (23):

$$(G_0)_{\max} = \frac{\left(\frac{f_{20}}{f_{10}}\right)}{\left[\sqrt{1 + \frac{f_{10}f_{20}}{M^2}} + \frac{\sqrt{f_{10}f_{20}}}{M}\right]^2}$$

$$\approx \frac{\left(\frac{f_{20}}{f_{10}}\right)}{1 + \frac{2\sqrt{f_{10}f_{20}}}{M}}, \quad M \gg \sqrt{f_{10}f_{20}}$$

$$(T_{e,0})_{\min} = 2\left(\frac{f_{10}}{M}\right)\left(\sqrt{1 + \frac{f_{10}^2}{M^2}} + \frac{f_{10}}{M}\right) T_D$$

$$\approx 2\left(\frac{f_{10}}{M}\right) T_D, \quad M \gg f_{10}.$$

Thus, the finite figure of merit M both lowers the gain below the ideal value equal to the frequency ratio and raises the noise temperature above the ideal value of zero. It is interesting to note that the minimum temperature, which is independent of the pump frequency, is identically equal to the minimum noise temperature of a one-port difference-frequency parametric amplifier with an optimum pump frequency [2].

An exact analysis for calculating the tunability with a lumped, single-tuned signal input circuit is given in Appendix II-A. A measure of the tunability, however,

can be gotten from the approximate 3-dB bandwidth of the signal input circuit (45). Tunability can theoretically be increased, at the cost of greater complexity, by using a multiple-tuned signal input circuit [1].

Table I summarizes typical predicted up-converter performance at the middle of the two frequency channels. Three different values of S_1, the unpumped midband signal input SWR, are used for each channel to calculate the midband effective input noise temperature relative to the varactor temperature (19), the midband available power gain (18), and the approximate fractional signal circuit bandwidth (45). These values of S_1 are the value for maximum gain (20), the value for minimum noise temperature (21), and the measured value in an actual converter. Listed at the bottom of Table I are the necessary room temperature parameter values used in making the calculations. It can be seen that the noise temperature and gain vary only slightly about their optimum values, but that the signal input circuit bandwidth (and hence, converter tunability) increases steadily with input SWR. Generally, the two channels are designed to achieve greater tunability at a very slight cost in noise temperature and a slightly greater cost in gain. For a 20 to 30°K range of up-converter physical temperature, the predicted noise temperatures are about 3 to 5°K, assuming no degradation in the varactor figure of merit from its room temperature value. On the other hand, circuit losses, which are neglected in Table I, should be even less at cryogenic temperatures.

Figure 4 shows measured transducer power gain for both frequency channels at room temperature vs. signal input frequency. This data was obtained from insertion-type measurements made with a constant signal input level from a well-matched signal generator, and a flat, well-matched detector preceded by appropriate filtering to avoid affecting the detector sensitivity with either fundamental or second harmonic pump leakage. Both up-converter and down-converter gain are shown.[1] Also included is the net gain (actually a loss) of the combined up-converter and down-converter for each channel. This loss of about 4 to 6 dB must be made up by the maser to achieve the desired minimum overall system gain.

Two comparisons with the theoretical performance of Table I can be made from Fig. 4. First, the measured midband up-converter gains are about 1 dB less than predicted. Second, the measured tunability is somewhat less than the approximate theoretical value indicated by the dotted lines. Among the likely reasons for these discrepancies are: 1) a slight mistuning of the signal input and sum output circuits, 2) the neglecting of circuit losses, especially bias circuit losses in Table I, 3) not correcting for the small output mismatch loss, 4) too little correction for the small filter loss in the filter preceding the detector, and 5) the distributed nature of the actual signal input circuit (with regard to the limited tunability). Other possible sources of error are imperfect flatness of the detector and a slightly high estimate of the varactor figure of merit ($M=30$ GHz). Subsequent measurements and calculations, however, do not support these latter hypotheses.

For completeness, Appendix I also includes a derivation of gain and noise temperature for operation as a down-converter [see (31), (32), and (33)]. A very general theoretical result is shown (34) for the ratio of up-converter and down-converter transducer power gains. This is plotted in Fig. 5 along with measured data from Fig. 4. It is seen that the measured points generally fall around the theoretical curve. An important fact to be deduced from this agreement is that the detector was indeed generally flat at the signal input and sum output frequencies. Thus, if the detector were δ dB more sensitive at f_1 than at f_{20}, the indicated up-converter gain would be low by δ dB, and the indicated down-converter gain would be high by δ dB. The resultant points in Fig. 5 would thus be generally shifted below the theoretical curve by 2δ dB. Since no such shift was observed, we can conclude that the detector was flat as stated.

Also included in Appendix I are a pair of dual relationships (29) and (30) between pumped and unpumped midband SWR at signal input and sum output ports. Table II compares measured and theoretical values of pumped SWR. The very good agreement evident serves as a check on the estimated value of varactor figure of merit ($M=30$ GHz), since the theoretical values of pumped SWR vary approximately inversely with the square of M.

The final experimental converter data to be presented is a plot of available pump power from a triode source vs. pump frequency (Fig. 6). The very wide range of pump frequency for which the power required to pump the varactors is less than 30 mW is evidence of the broadbanding of the pump tuning. This is accomplished by tuning as closely as possible to the varactors in a very overcoupled single-tuned circuit.[2] Of the 9-mW mid-range pump power required, it is estimated that only about 2 mW is actually dissipated in the varactors. These measurements were made at room temperature with -1 volt bias applied to the varactors and 1 μA of total rectified current flowing. This operating point, which was also used in the previously described gain and SWR measurements, is nearly optimum at room temperature in the sense that conversion gain (either up or down) attains a broad maximum in its vicinity. The equivalent operating point for the up-converter at a physical temperature of about 25°K is near zero bias while pumping at a level just below that which causes a barely perceptible rectified current reading.

[1] At the normal cryogenic operating temperature of the up-converter, the gain was about 0.3 dB less than that shown in Fig. 4.

[2] This contrasts with the multiple-tuned approach to pump tuning described in Reference [1].

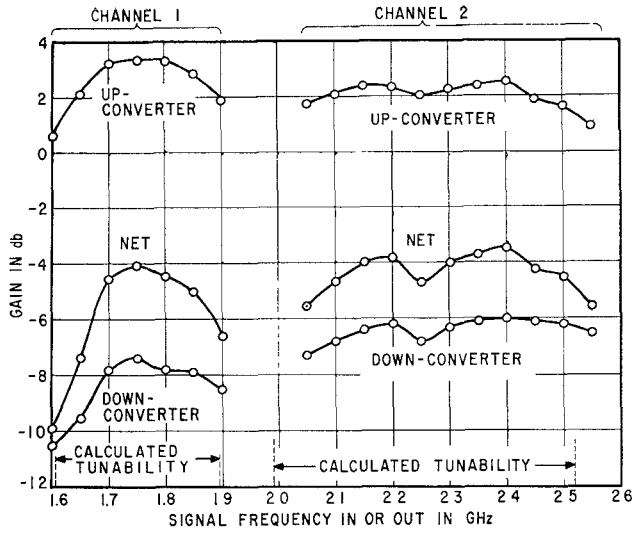

Fig. 4. Converter tunability (gain vs. signal frequency at room temperature).

TABLE I

THEORETICAL PERFORMANCE VS. SIGNAL CIRCUIT TRANSFORMATION

f_{10}	S_1	T_e/T_D (theor)	G (theor)	$1/Q_1$ (theor)
1.75 GHz	9.3	0.142	4.42 dB (max)	0.100
	16.0 (meas)	0.125	4.30 dB	0.165
	17.2	0.124 (min)	4.27 dB	0.177
2.25 GHz	8.2	0.181	3.20 dB (max)	0.115
	13.4	0.162 (min)	3.10 dB	0.180
	18.0 (meas)	0.167	2.94 dB	0.237

Assumed parameters: $f_{20}=6$ GHz, $M=30$ GHz, $f_c=120$ GHz, $C_p/C_0^s=0.5$.

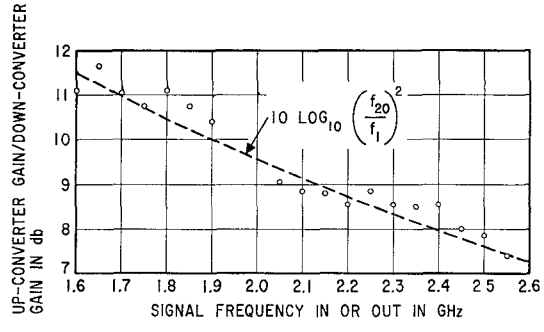

Fig. 5. Gain ratio of up-converter and down-converter vs. signal frequency.

TABLE II

PUMPED AND UNPUMPED SWR VALUES

f_{10}	S_1 (meas)	S_2 (meas)	S_1 (pumped)	S_2 (pumped)
1.75 GHz	16	4.7	1.53 (meas)	$\frac{1}{1.11}$ (meas)
			1.00 (theor)	$\frac{1}{1.28}$ (theor)
2.25 GHz	18	5.3	1.36 (meas)	$\frac{1}{1.33}$ (meas)
			1.55 (theor)	1.18 (theor)

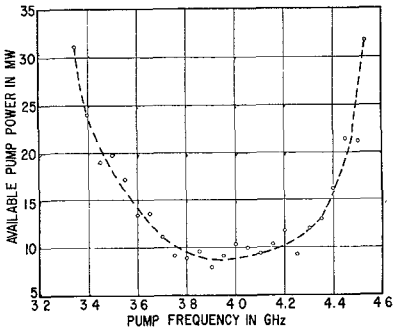

Fig. 6. Pump power vs. pump frequency.

III. TRAVELING-WAVE MASER

A. General

The output signal from the varactor up-converter is fed to the second-stage traveling-wave maser (TWM), Fig. 1. Whereas the up-converter is a widely tunable, low-noise low-gain amplifier, the TWM is a high-gain, broadband low-noise amplifier. In this application, the TWM is fixed tuned and the up-converter down-converter combination is tuned to cover the desired frequency band. The maser amplifier employs a comb-type slow-wave structure, single crystal ruby ($\theta=90°$) as the active material, and YIG disk isolators for stability.

B. Selection of Maser Frequency

Initial converter and maser design centered the sum frequency in the C-band region. Final selection of a 6 GHz maser frequency was determined by spurious response considerations.

Figure 7 is a generalized graphical representation of the possible spurious responses which might be produced as a function of signal frequency normalized to the sum frequency. From Fig. 7, it can be seen that $f_1/f_2=0.25$, 0.33, and 0.4 are operating points which have lower order spurious responses. As a result, the signal bands and sum frequency were chosen to avoid these potentially troublesome modes. The signal bands were centered at 1750 and 2250 MHz and the maser (sum) frequency was fixed at 6000 MHz.

Figure 8 shows the closest lower order spurious responses for the system operating parameters as determined from Fig. 7. Only lower order signal harmonics ($|m|<4$) are considered since a low-level signal is employed. In addition, the balanced circuit configuration of the up-converter suppresses spurious modes having even values of n. The sum frequency operating mode ($m=1$, $n=1$) is shown as a solid line running from upper left to lower right, and pump frequencies corresponding to the two signal channels lie between the pairs of horizontal slashed lines. The intersections of these slashed lines with the 3 spurious modes shown determine the closest potentially troublesome spurious signal responses.

C. Amplifier Characteristics

Identical low-noise TWM's are used as the second stage in each channel. The masers are centered near

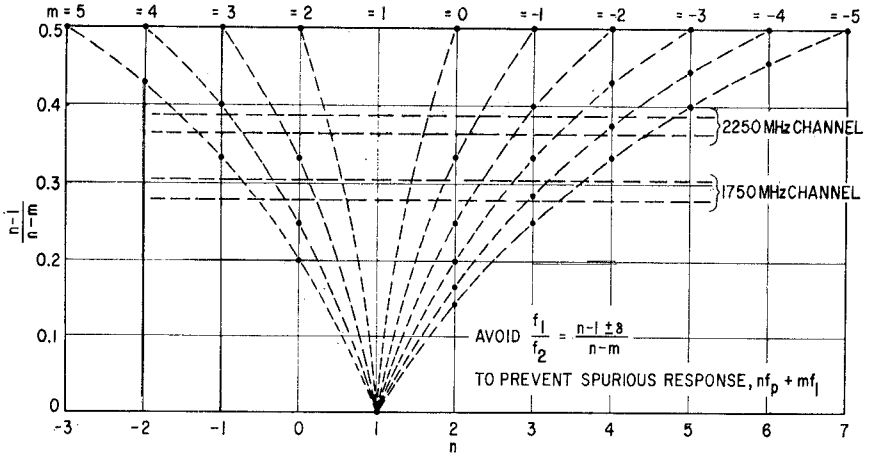

Fig. 7. General spurious response considerations.

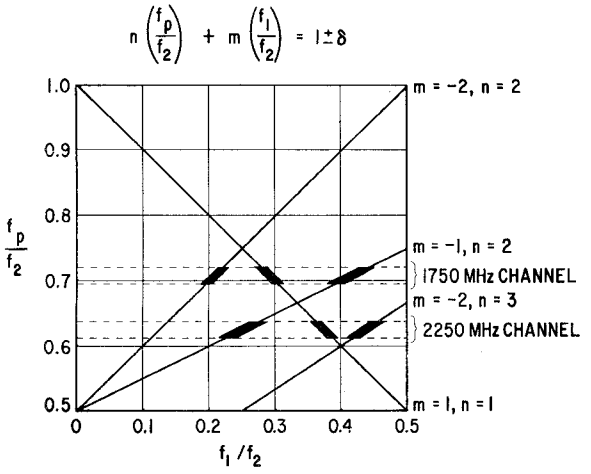

Fig. 8. Closest spurious responses.

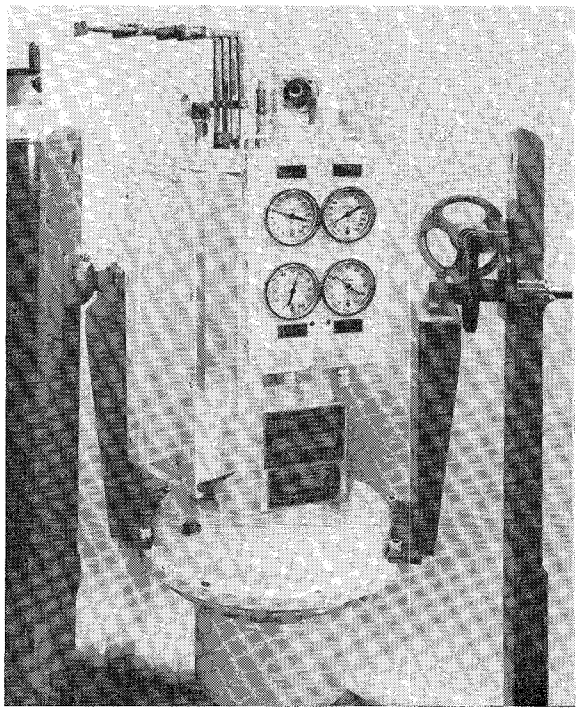

Fig. 9. Closed-cycle refrigerator.

6000 MHz and have a gain of 36 dB. The instantaneous maser bandwidth is 70 MHz, and is obtained by using transverse magnetic field staggering techniques [3]. By providing for some maser tuning, potentially troublesome spurious modes can be avoided and noise performance optimized.

Ferrite (YIG) disks are incorporated into the slow-wave structure. The disks, which have a reverse-to-forward magnetic loss ratio of 35:1, have a reverse loss of greater than 90 dB per channel—resulting in unconditionally stable TWM's. A pair of ITT type 2900 reflex klystrons centered near 36 GHz are used to pump the two masers. The required magnetic field of approximately 4000 gauss is provided by a conductively cooled superconducting magnet. The magnet is made up of two sections of Nb 25 Zn wire wound on an 8-inch aluminum form.

The TWM's and superconducting magnet are conductively cooled to approximately 4.2°K by an ADL Model 400 closed-cycle refrigerator (Fig. 9). The up-converters are cooled to a temperature of approximately 27°K using the same refrigerator.

IV. Coupled Up-Converter-Maser System Data

Preliminary measurements on the up-converter-maser combinations have resulted in low-noise system performance over an 800 MHz tuning range. Figure 10 shows the measured noise temperatures for channels I and II. For channel I, the measured overall noise temperature was less than 25°K over a 200 MHz range and less than 30°K over a 325 MHz range. The dashed curve is the measured data corrected for an estimated 8°K contribution of the input line. For channel II, the measured overall noise temperature was less than 30°K over a 250 MHz band. The original measurement for channel II was made with a breadboard 15°K input line, but the data has been adjusted to reflect the improved input lines. It is expected that the noise contribution due to the input line loss could be reduced further (3 to 5°K) by going to larger gold plated input lines.

As expected, the minimum noise temperature for each

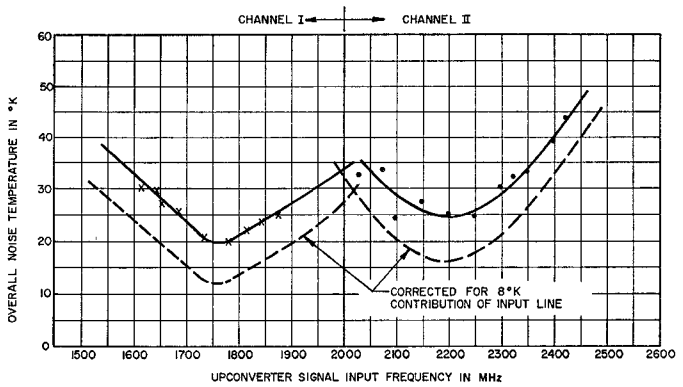

Fig. 10. Measured noise temperature of up-converter maser system vs. signal frequency (up-converter physical temperature $\approx 30°K$).

channel is at the design center of the channel. The noise temperature degradation at the band edges is attributable to the effect of changing signal circuit impedance on up-converter noise temperature (17), gain (16), and output impedance (11). The latter two effects degrade the overall noise temperature by increasing the noise contributions of the maser and its input line.

The system gain is 30 dB per channel and the instantaneous bandwidth is presently determined by the maser bandwidth (≈ 70 MHz). For applications where larger instantaneous bandwidths are required, the TWM could be replaced with a cooled circulator-coupled one-port parametric amplifier with a resulting degradation in system noise performance.

This data is still preliminary and complete system data will be reported when it becomes available.

Appendix I

Power Gain and Effective Input Noise Temperature of Lossy Parametric Converter

A. Up-Converter

The equivalent circuit of the sum frequency parametric up-converter including varactor loss is shown in Fig. 11. The overall circuit is divided into five individual networks connected in cascade. These are:

1) a lossless network at signal input frequency f_1 that includes the pumped average-series capacitance C_0^s [1], and the parasitic reactances[3] of the varactor, as well as external reactive tuning and impedance transforming elements. This network is characterized by its output impedance $Z_1 = R_1 + jX_1$, and does not contribute directly to the gain or noise temperature of the up-converter.
2) A network (number 1) that gives the effect of the series varactor loss resistance (R_s at physical temperature T_D) at signal frequency f_1.
3) A network (number 2) that represents an ideal lossless up-converter with applied pump frequency f_p. (The $X_{12}X_{21}$, notation of Reference [1] is used.) The output impedance of network 2 is denoted by $Z_{out,2}$.
4) A network (number 3) that gives the effect of the series varactor loss resistance (R_s at physical temperature T_D) at sum frequency f_2.
5) A lossless network at sum frequency f_2 that includes the pumped average series capacitance C_0^s and the parasitic reactances of the varactor, as well as external reactive tuning and impedance transforming elements. This network is characterized by its input impedance $Z_2 = R_2 + jX_2$, and does not contribute directly to the available power gain or noise temperature of the up-converter. However, any mismatch associated with impedance Z_2 will affect the maser second stage contribution to the overall system gain and noise temperature.

[3] At the signal input frequency, the main parasitic reactance is the package capacitance C_p.

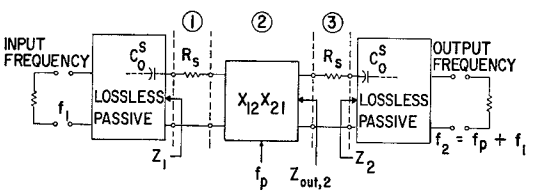

Fig. 11. Equivalent cascaded networks for analysis of lossy sum frequency parametric amplifier.

Attention will be fixed on a constant midband output sum frequency $f_2 = f_{20}$, corresponding to the center frequency of the relatively narrow-band second stage. For this condition, $Z_2 = R_{20} + j0$. Then, as the up-converter pump frequency (f_p) is varied, the available power gain (G) and the effective input noise temperature (T_e) of the up-converter will be determined as functions of the variable signal frequency f_1 by using the cascaded network relations [4]:

$$G = G_1 G_2 G_3 \tag{1}$$

$$T_e = T_{e1} + \frac{T_{e2}}{G_1} + \frac{T_{e3}}{G_1 G_2}. \tag{2}$$

In (1) and (2), the effective input noise temperature T_e is related to the noise factor F and the reference temperature T_0 by

$$T_e = (F - 1)T_0, \tag{3}$$

and subscripts 1 through 3 refer to the corresponding networks in Fig. 11.

Next, consider the individual networks 1 through 3. From the definitions in Reference [4], it is readily shown for network 1 that

$$G_1 = \frac{S_1\left(\frac{R_1}{R_{10}}\right)}{S_1\left(\frac{R_1}{R_{10}}\right) + 1} \tag{4}$$

$$T_{e1} = \frac{T_D}{S_1\left(\frac{R_1}{R_{10}}\right)} \tag{5}$$

where

$$S_1 \text{ (parameter } T \text{ in Reference [1])} = \frac{R_{10}}{R_s} \tag{6}$$

and R_{10} is the midband (that is, center of the tuning range) value of R_1. Note that since the midband value of $X_1 = X_{10} = 0$, S_1 is the unpumped midband input SWR that would be measured with the varactor biased for a small-signal capacitance equal to C_0.[4]

From the Manley-Rowe basic power relations [5], and neglecting possible noise sources such as shot noise, we obtain for network 2

$$G_2 = \frac{f_{20}}{f_1} \tag{7}$$

$$T_{e2} = 0. \tag{8}$$

For network 3, in a manner analogous to that for network 1, we obtain

$$G_3 = \frac{1}{1 + \frac{R_s}{\text{Re}\,[Z_{\text{out, 2}}]}} \tag{9}$$

$$T_{e3} = \frac{R_s T_D}{\text{Re}\,[Z_{\text{out, 2}}]}. \tag{10}$$

From the impedance inverting property of the lossless up-converter [1], the output impedance of network 2 is

$$Z_{\text{out, 2}} = \frac{X_{12}X_{21}}{R_1 + R_s + jX_1} = \frac{R_s\left(\frac{M^2}{f_1 f_{20}}\right)}{S_1\left(\frac{R_1}{R_{10}}\right) + 1 + j\left(\frac{X_1}{R_s}\right)} \tag{11}$$

where

$$M \text{ (varactor figure of merit)} = f_c\left(\frac{C_1}{C_0}\right), \tag{12}$$

$$f_c \text{ (varactor cutoff frequency)} = \frac{1}{2\pi R_s C_0}, \tag{13}$$

and C_1/C_0 = varactor capacitance nonlinearity [1]. Equations (9) and (10) thus become

$$G_3 = \frac{\frac{M^2}{f_1 f_{20}}\left[S_1\left(\frac{R_1}{R_{10}}\right) + 1\right]}{\frac{M^2}{f_1 f_{20}}\left[S_1\left(\frac{R_1}{R_{10}}\right) + 1\right] + \left[S_1\left(\frac{R_1}{R_{10}}\right) + 1\right]^2 + \left[\frac{X_1}{R_s}\right]^2} \tag{14}$$

$$T_{e3} = \frac{\left\{\left[S_1\left(\frac{R_1}{R_{10}}\right) + 1\right]^2 + \left[\frac{X_1}{R_s}\right]^2\right\} T_D}{\frac{M^2}{f_1 f_{20}}\left[S_1\left(\frac{R_1}{R_{10}}\right) + 1\right]}. \tag{15}$$

Finally, the desired results for gain and noise temperature are obtained by substituting (4), (5), (7), (8), (14), and (15), into (1) and (2). The results are

$$G = \frac{\left(\frac{f_{20}}{f_1}\right)}{\left[1 + \frac{1}{S_1\left(\frac{R_1}{R_{10}}\right)}\right]\left[1 + \frac{f_1 f_{20}}{M^2}\left\{S_1\left(\frac{R_1}{R_{10}}\right) + 1\right\}\left\{1 + \frac{\left[\frac{X_1}{R_s}\right]^2}{\left[S_1\left(\frac{R_1}{R_{10}}\right) + 1\right]^2}\right\}\right]} \tag{16}$$

$$T_e = \frac{T_D}{S_1\left(\frac{R_1}{R_{10}}\right)}\left(1 + \frac{f_1^2}{M^2}\left\{\left[S_1\left(\frac{R_1}{R_{10}}\right) + 1\right]^2 + \left[\frac{X_1}{R_s}\right]^2\right\}\right). \tag{17}$$

[4] It is assumed that the usual condition $R_{10}/R_s > 1$ is satisfied. Otherwise, the input SWR equals $1/S_1$.

Under midband conditions ($f_1=f_{10}$, $R_1=R_{10}$, $X_1=0$), (16) and (17) reduce to[5]

$$G_0 = \frac{\left(\frac{f_{20}}{f_{10}}\right)}{\left[1+\frac{1}{S_1}\right]\left[1+\frac{f_{10}f_{20}}{M^2}(S_1+1)\right]} \tag{18}$$

$$T_{e,0} = \frac{T_D}{S_1}\left[1+\frac{f_{10}^2}{M^2}(S_1+1)^2\right]$$

$$= \left\{\left[1+\frac{1}{S_1}\right]\left[1+\frac{f_{10}^2}{M^2}(S_1+1)\right]-1\right\}T_D. \tag{19}$$

It can be seen that optimum values of S_1 exist to maximize the midband gain or to minimize the midband noise temperature. These values are, respectively,

$$(S_1)_{\text{opt, 1}} = \sqrt{\frac{M^2}{f_{10}f_{20}}+1} \tag{20}$$

and

$$(S_1)_{\text{opt, 2}} = \sqrt{\frac{M^2}{f_{10}^2}+1} > (S_1)_{\text{opt, 1}}. \tag{21}$$

The corresponding values of maximum midband gain and minimum midband noise temperature are

$$(G_0)_{\max} = \frac{\left(\frac{f_{20}}{f_{10}}\right)}{\left[\sqrt{1+\frac{f_{10}f_{20}}{M^2}}+\frac{\sqrt{f_{10}f_{20}}}{M}\right]^2} \tag{22}$$

$$(T_{e,0})_{\min} = 2\left(\frac{f_{10}}{M}\right)\left(\sqrt{1+\frac{f_{10}^2}{M^2}}+\frac{f_{10}}{M}\right)T_D. \tag{23}$$

It is also of interest to derive the transducer power gain G_t with the actual load and express the result as a function of unpumped midband output SWR. The transducer gain is related to the available power gain by

$$G_t = [1-|\Gamma_{\text{out, 3}}|^2]G \tag{24}$$

where $\Gamma_{\text{out, 3}}$, the reflection coefficient at the output of network 3, is given by [6].

$$\Gamma_{\text{out, 3}} = \frac{Z_2-(R_s+Z_{\text{out, 2}})^*}{Z_2+R_s+Z_{\text{out, 2}}}. \tag{25}$$

Substitution of (11) and (25) into (24) then gives

$$G_t = \frac{4S_1S_2\left(\frac{R_1}{R_{10}}\right)\left(\frac{M}{f_1}\right)^2}{\left\{\frac{M^2}{f_1f_{20}}+\left[S_1\left(\frac{R_1}{R_{10}}\right)+1\right][S_2+1]\right\}^2+\left\{(S_2+1)\left(\frac{X_1}{R_s}\right)\right\}^2} \tag{26}$$

where S_2, the unpumped midband output SWR (analogous to S_1, the unpumped midband input SWR), is

$$S_2 = \frac{R_{20}}{R_s}. \tag{27}$$

At midband, the transducer power gain reduces to

$$G_{t,0} = \frac{4S_1S_2\left(\frac{M}{f_{10}}\right)^2}{\left[\frac{M^2}{f_{10}f_{20}}+(S_1+1)(S_2+1)\right]^2}. \tag{28}$$

An interesting dual relationship exists between the pumped and unpumped midband SWR at the input and output ports. From (25) and (11), the pumped midband output SWR is[6]

$$(S_2)_{\text{pumped}} = \frac{1+|\Gamma_{\text{out, 3}}|_0}{1-|\Gamma_{\text{out, 3}}|_0} = \frac{S_2}{1+\left(\frac{M^2}{f_{10}f_{20}}\right)\left(\frac{1}{S_1+1}\right)}. \tag{29}$$

Similarly, the pumped midband input SWR can be derived, and is

$$(S_1)_{\text{pumped}} = \frac{S_1}{1+\left(\frac{M^2}{f_{10}f_{20}}\right)\left(\frac{1}{S_2+1}\right)}. \tag{30}$$

B. Down-Converter

For the down-converter, the equivalent circuit of Fig. 11 applies with the input signal frequency (f_{20}) applied to the port marked "load" and the output signal frequency (f_1) taken from the port marked "source." Analyzing exactly as in Part A leads to the following results for available power gain (actually a loss) and effective input noise temperature:

$$G = \frac{\left(\frac{f_1}{f_{20}}\right)}{\left[1+\frac{1}{S_2}\right]\left[1+\frac{f_1f_{20}}{M^2}(S_2+1)\right]} < 1 \tag{31}$$

$$T_e = \frac{T_D}{S_2}\left[1+\frac{f_{20}^2}{M^2}(S_2+1)^2\right]. \tag{32}$$

[5] Equation (18) is the same as (28) of Reference [1], ($f_{10}f_{20}/M^2=v^2$).

[6] It is assumed that $(S_2)_{\text{pumped}}>1$; otherwise the pumped midband output SWR equals $1/(S_2)_{\text{pumped}}$, and similarly for $(S_1)_{\text{pumped}}$.

Note that, at midband, these formulas are the same as for the up-converter (18) and (19) with f_{10} and f_{20} as well as S_1 and S_2 interchanged.

It is also of interest to derive the transducer power gain for the down-converter. In a manner similar to that used for the up-converter in Part A, the transducer gain for the down-converter is found to be

$$G_t = \frac{4S_1S_2\left(\frac{R_1}{R_{10}}\right)\left(\frac{M}{f_{20}}\right)^2}{\left\{\frac{M^2}{f_1f_{20}} + \left[S_1\left(\frac{R_1}{R_{10}}\right)+1\right][S_2+1]\right\}^2 + \left\{(S_2+1)\left(\frac{X_1}{R_s}\right)\right\}^2}. \tag{33}$$

Comparing (33) and (26) leads to the interesting general result that the ratio of the transducer power gains for the same noninverting lossy parametric converter operated as an up-converter or as a down-converter is independent of everything except the frequencies involved:

$$\frac{(G_t)_{UC}}{(G_t)_{DC}} = \left(\frac{f_{20}}{f_1}\right)^2. \tag{34}$$

Appendix II

Application to a Lumped, Single-Tuned Signal Input Circuit

Calculation of the up-converter gain and noise temperature performance over a range of signal frequencies using the results of Appendix I, requires a knowledge of the specific signal circuit through the parameters R_1 and X_1 [see (16), (17), and (26)]. The simplest signal circuit to analyze (and also to build) is the lumped single-tuned circuit (Fig. 12). Included in Fig. 12 are the pumped average series varactor capacitance C_0^s, a lumped tuning inductance L_1, the effective generator resistance R_0, and (because of its importance) the varactor package capacitance C_p. This circuit has been analyzed exactly and approximately.

A. Exact Analysis

Straightforward network analysis gives (after some algebraic manipulation) for the real and imaginary parts of the effective signal source impedance $Z_1 = R_1 + jX_1$,

$$R_1 = \frac{R_0}{(1-\omega_1^2L_1C_p)^2 + \omega_1^2C_p^2R_0^2} \tag{35}$$

$$X_1 = \frac{\omega_1L_1 - \omega_1C_p(R_0^2+\omega_1^2L_1^2)}{(1-\omega_1^2L_1C_p)^2 + \omega_1^2C_p^2R_0^2} - \frac{1}{\omega_1C_0^s} \tag{36}$$

where the angular signal frequency $\omega_1 = 2\pi f_1$.

A similar procedure gives relations for the generator resistance and tuning inductance to satisfy the midband conditions ($R_1 = R_{10} = S_1R_s$ and $X_1 = 0$ at $\omega_1 = \omega_{10}$):

$$\frac{R_0}{R_{10}} = \frac{1}{\left(1+\frac{C_p}{C_0^s}\right)^2 + \left(\frac{C_p}{C_0^s}\right)^2 D_0^2} \tag{37}$$

$$\omega_{10}^2L_1C_0^s = \frac{1+\frac{C_p}{C_0^s}+\left(\frac{C_p}{C_0^s}\right)D_0^2}{\left(1+\frac{C_p}{C_0^s}\right)^2 + \left(\frac{C_p}{C_0^s}\right)^2 D_0^2} \tag{38}$$

where

$$D_0 = \omega_{10}C_0^sR_{10} = S_1\left(\frac{f_{10}}{f_c}\right). \tag{39}$$

Substitution of (37) and (38) into (35) and (36) then gives desired result (after much algebraic manipulation),

$$\frac{R_1}{R_{10}} = \frac{\left(1+\frac{C_p}{C_0^s}\right)^2 + \left(\frac{C_p}{C_0^s}\right)^2 D_0^2}{\left[1+\frac{C_p}{C_0^s} - \frac{C_p}{C_0^s}\left(\frac{f_1^2}{f_{10}^2}-1\right)\left(1+\frac{C_p}{C_0^s}+\frac{C_p}{C_0^s}D_0^2\right)\right]^2 + \left(\frac{f_1}{f_{10}}\right)^2\left(\frac{C_p}{C_0^s}\right)^2 D_0^2} \tag{40}$$

$$\frac{X_1}{R_0} = \frac{\frac{f_c}{f_{10}}\left\{\frac{f_1}{f_{10}} - \frac{f_{10}}{f_1}\right\}\left\{\left[1+\frac{C_p}{C_0^s}\right]^3 - \left(\frac{C_p}{C_0^s}\right)^3 D_0^4 - \frac{C_p}{C_0^s}\left[\frac{f_1^2}{f_{10}^2}-1\right]\left[1+\frac{C_p}{C_0^s}\right]\left[1+\frac{C_p}{C_0^s}(1+D_0^2)\right]^2\right\}}{\left[1+\frac{C_p}{C_0^s} - \frac{C_p}{C_0^s}\left(\frac{f_1^2}{f_{10}^2}-1\right)\left(1+\frac{C_p}{C_0^s}+\frac{C_p}{C_0^s}D_0^2\right)\right]^2 + \left(\frac{f_1}{f_{10}}\right)^2\left(\frac{C_p}{C_0^s}\right)^2 D_0^2}. \tag{41}$$

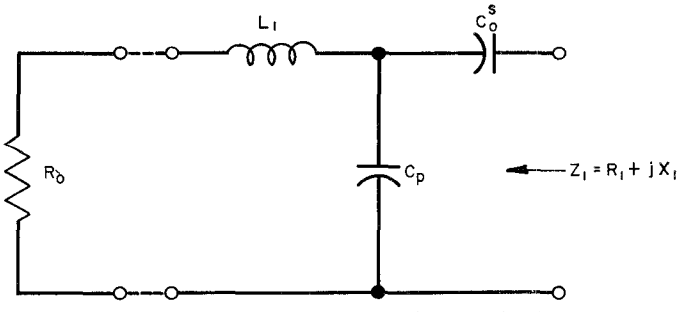

Fig. 12. Lumped single-tuned signal circuit.

Exact calculations of gain and noise temperature vs. signal input frequency can then be made using (40), (41), (16), (17), and (26).

B. Approximate Analysis

For the approximate analysis, the assumption is made that the tuning range of signal input frequency is roughly equal to the loaded signal circuit 3-dB bandwidth. This bandwidth is in turn calculated approximately as follows. The complete signal circuit loop impedance in Fig. 11 is

$$Z_{\text{loop}} = Z_1 + R_s = R_1 + R_s + jX_1. \tag{42}$$

The fractional loaded signal circuit 3-dB bandwidth is then

$$\frac{(\Delta f_1)_{3\text{ dB}}}{f_{10}} = \frac{1}{Q_1} \approx \frac{2(R_{10} + R_s)}{\omega_{10}\left(\frac{dX_1}{d\omega_1}\right)_{\omega_1=\omega_{10}}}. \tag{43}$$

From (41) and (6), (43) becomes

$$\frac{(\Delta f_1)_{3\text{ dB}}}{f_{10}} \approx \frac{f_{10}(S_1+1)}{f_c}\left[\frac{\left(1+\frac{C_p}{C_0{}^s}\right)^2 + D_0{}^2\left(\frac{C_p}{C_0{}^s}\right)^2}{\left(1+\frac{C_p}{C_0{}^s}\right)^3 - D_0{}^4\left(\frac{C_p}{C_0{}^s}\right)^3}\right]. \tag{44}$$

A further approximation can be made if $\omega_{10}C_pR_{10} \ll 1 + (C_p/C_0{}^s)$ and $D_0 < 1$, namely

$$\frac{(\Delta f_1)_{3\text{ dB}}}{f_{10}} \approx \frac{f_{10}(S_1 + 1)}{f_c\left(1 + \frac{C_p}{C_0{}^s}\right)}. \tag{45}$$

Acknowledgment

The authors wish to thank P. Lombardo and J. DeGruyl for technical discussions on the design of the converter and maser, respectively. They also wish to thank J. Wolczok, R. Lange, A. Kunze, E. Barnell, and H. Gable for their technical assistance.

References

[1] G. L. Matthaei, "Design theory of up-converters for use as electronically-tunable filters," *IRE Trans. on Microwave Theory and Techniques*, vol. MTT-9, pp. 425–435, September 1961.

[2] J. C. Greene and E. W. Sard, "Optimum noise and gain-bandwidth performance for a practical one-port parametric amplifier," *Proc. IRE*, vol. 48, pp. 1583–1590, September 1960.

[3] J. A. De Gruyl, S. Okwit, and J. G. Smith, "Techniques for providing TWM's with wide instantaneous bandwidths," *1965 G-MTT Symp. Digest*, pp. 193–197.

[4] H. T. Friis, "Noise figures of radio receivers," *Proc. IRE*, vol. 32, pp. 419–422, July 1944.

[5] J. M. Manley and H. E. Rowe, "Some general properties of nonlinear elements. Part I, General energy relations," *Proc. IRE*, vol. 44, pp. 904–913, July 1956.

[6] H. W. Bode, *Network Analysis and Feedback Amplifier Design*. New York: Van Nostrand, 1945, p. 364.

Improved Intermodulation Rejection in Mixers

J. H. LEPOFF, SENIOR MEMBER, IEEE, AND A. M. COWLEY, MEMBER, IEEE

***Abstract*—Intermodulation is one of the most pernicious forms of spurious response in superheterodyne receivers. This type of interference cannot be completely eliminated by narrowband filters. Improvements in receiver performance can be made only by improving and making more effective use of the mixing element.**

Intermodulation results from terms of higher order than two in the *v-i* power series expansion about the dc operating point of the mixing element. The magnitude of these higher order terms must be reduced in order to improve intermodulation rejection. In the work described in this paper, it has been observed that such a reduction in higher order terms can be obtained by proper design of the mixing element and by a proper choice of dc operating point.

More than 80 dB intermodulation rejection was obtained with a single ended hot carrier diode mixer. Best performance is obtained by operating two hot carrier diodes at different operating points in a balanced mixer arrangement. Intermodulation ratios greater than 100 dB have been measured for this operating mode. Optimization of performance for IM rejection has little effect on sensitivity or rejection of other spurious responses.

A new mixing element, the space-charge-limited resistor (SCLR), was designed to minimize the higher order terms in the current function. A balanced mixer provided the best performance with these mixing elements also. Intermodulation from +5 dBm inputs can be rejected below the mixer noise level. Early models of this device are not as sensitive as hot carrier mixers, but improvement appears to be possible.

Manuscript received June 13, 1966; revised August 2, 1966. This work was supported by the U. S. Air Force Systems Command under Contract AF 33 (615)-2600.

The authors are with -hp- Associates, Palo Alto, Calif.

Introduction

THE INCREASING spectrum density of electromagnetic radiation has stimulated an interest in receivers which do not respond to signals which are not separated from the local oscillator frequency by the intermediate frequency. Such spurious responses result from combinations of harmonics of incoming signals with harmonics of the local oscillator. The general expression for two spurious input frequencies, f_1 and f_2, is

$$mf_2 - nf_1 = pf_{\text{LO}} \pm f_{\text{IF}}.$$